

Do the environmental conditions affect the dust-induced fragmentation in low-metallicity clouds?: Effect of pre-ionization and far-ultraviolet/cosmic-ray fields

Kazuyuki OMUKAI

Department of Physics, Kyoto University, Kyoto 606-8502, Japan
omukai@tap.scphys.kyoto-u.ac.jp

(Received ; accepted)

Abstract

We study effects of the fully ionized initial state, or pre-ionization, on the subsequent thermal evolution of low-metallicity clouds under various intensities of the external far-ultraviolet(FUV) and cosmic-ray(CR) fields. The pre-ionization significantly affects the thermal and dynamical evolution of metal-free clouds without FUV/CRs by way of efficient HD formation. On the other hand, the pre-ionization effect on the thermal evolution is limited in very low-density regime for more metal-enriched clouds ($[Z/H] \gtrsim -4$) or those under modest FUV ($\gtrsim 10^{-3}$) or CR field ($\gtrsim 0.1$ of the present-day Galactic disk levels). In any case, for $\gtrsim 10^8 \text{cm}^{-3}$, neither the initial ionization state nor the irradiating FUV strength affect the thermal evolution. The dust cooling is an important mechanism for making sub-solar mass fragments in low-metallicity gas. Since this fragmentation occurs at the temperature minimum by the dust cooling at $\gtrsim 10^{10} \text{cm}^{-3}$, this process is not vulnerable either to initial ionization state or external radiation.

Key words: stars: formation — stars: Population II — ISM: molecules

1. Introduction

The first generation of stars, or the so-called population III.1 stars (pop III.1 stars; O’Shea et al. 2008), are formed out of the primordial pristine gas with a small ionization degree ($\sim 10^{-4}$) left from the cosmic recombination (Peebles 1968; Sasaki & Takahara 1993). Within mini-halos with $\gtrsim 10^6 M_\odot$, the collapse of primordial clouds is induced by the H_2 cooling, which sets a characteristic mass-scale of dense cores at several $100 M_\odot$ (Bromm, Coppi, & Larson 1999; Abel, Bryan, & Norman 2002). Inside these cores, protostars eventually form as a result of further gravitational collapse by the H_2 cooling (Omukai & Nishi 1998; Yoshida, Omukai, & Hernquist 2008). Although the exact value of final stellar mass is still elusive, it is speculated that the stars grow massive (\gtrsim several $10 M_\odot$) owing to combined effects of high accretion rate and low opacity in primordial gas (Omukai & Palla 2003; Bromm & Loeb 2004; McKee & Tan 2008; Hosokawa et al. 2011).

Despite with the same primordial composition, stars formed under influences of radiative/mechanical feedbacks from pre-existing stars are expected to have a different characteristic mass-scale from that of the pop III.1 stars, and thus the terminology of pop III.2 stars have been proposed to specify them (O’Shea et al. 2008). Among various feedback mechanisms, e.g., photodissociation by the stellar far-ultraviolet radiation (Omukai 2001; O’Shea & Norman 2008), the sweeping by supernova blast waves (Mackey, Bromm, & Hernquist 2003; Salvaterra, Ferrara, & Schneider 2004; Machida et al. 2005), one of the most well-studied is the case of star formation in relic HII regions of the first stars (O’Shea et al. 2005; Nagakura

& Omukai 2005; Machida, Omukai & Matsumoto 2009). The massive first stars ionize the surrounding material by UV radiation (e.g., Kitayama et al. 2004). Except two ranges ($10 - 40 M_\odot$ and $140 - 260 M_\odot$) in mass, they end their lives rather quietly without supernova explosions (Heger & Woosley 2002; Umeda & Nomoto 2002). In those relic HII regions, the recombination proceeds in timescale $\sim 10^8$ yrs and the gas condenses again to form next-generation stars (Yoshida et al. 2007). Such pre-ionized primordial-gas follows a different thermal evolution from the pristine primordial gas of pop III.1 star formation (Uehara & Inutsuka 2002; Nakamura & Umemura 2002). In the pre-ionized gas, more H_2 (with molecular fraction $\sim 10^{-2}$) than in the pristine gas ($\sim 10^{-3}$) forms via the electron-catalyzed reaction,



and thus its cooling lowers the temperature below the minimum attainable in the pristine gas ($\simeq 200\text{K}$). In such a cold gas, HD fractionation is strongly favored via the exothermic (with energy difference $\Delta E/k_B = 464\text{K}$) reaction



and the resultant HD cooling further lowers the temperature to a few tens K, close to the CMB temperature in the high-redshift universe, $T_{\text{CMB}} = 27.3\text{K}(1+z)/10$. Those HD-cooling clouds fragment into dense cores of a few $10 M_\odot$, which bear stars at their centers incorporating a large part of the material in the cores (Yoshida, Omukai & Hernquist 2007; McGreer & Bryan 2008). Namely, the

history of ionization in a low-density medium, or “pre-ionization”, has a large effect on the subsequent thermal evolution of the metal-free gas, and possibly changes the characteristic stellar mass.

For metal-enriched clouds, the pre-ionization effect has not been explored comprehensively so far. Some previous studies, though, indicate that it has indeed effects on the thermal evolution at least in some range of metallicity. For example, in the initially un-ionized cases with metallicity $[Z/H] \gtrsim -3.5$ ¹, cooling by fine-structure transitions of carbon and oxygen lowers the temperature below the minimum value attainable solely by the H₂ cooling in the pristine gas ($\simeq 200\text{K}$ at $\sim 10^4\text{cm}^{-3}$) (Omukai 2000; Bromm & Loeb 2003). On the other hand, from the pre-ionized initial condition, the minimum temperature attainable does not change so much from that in the primordial gas even for metallicity as much as $[Z/H] \sim -2$ (Jappsen et al. 2007).

The pre-ionization effect in the metal-free gas is largely due to the HD formation and cooling. HD is also known to be quite susceptible to irradiation of FUV as well as ionization by the cosmic rays. For example, even in the pre-ionized gas, existence of only a weak FUV field prevents HD formation and its cooling (Yoshida, Omukai, & Hernquist 2007b; Wolcott-Green & Haiman 2010). On the contrary, a certain amount of cosmic-ray (CR) irradiation (with a few % of the energy density in the present-day Galactic disk) enables HD formation/cooling in an initially un-ionized cloud (Stacy & Bromm 2007).

In this paper, we study whether the pre-ionization affects the subsequent thermal evolution of low-metallicity clouds under a variety of intensities of the external FUV and CR fields. We also aim to clarify the density range where the thermal evolution is influenced by the external FUV and CR irradiation. The current preferred theory expects that transition from the Pop III massive star formation mode to the Pop II/I low-mass star mode is caused by the modification of thermal evolution due to the accumulation of metals in the star-forming gas, albeit the exact value of the critical metallicity is still in dispute (Schneider et al. 2002; Bromm & Loeb 2003; Dopcke et al. 2011). However, if the influences of environmental parameters, e.g., pre-ionization or external radiation fields, remain until high density where the fragmentation and low-mass core formation occur, we also need to care about those parameters in studying fragmentation properties of low-metallicity clouds and thus the problem would become highly complex.

Our calculations here, fortunately, revealed that the pre-ionization alters the thermal evolution only in low density except cases with very low-metallicity ($[Z/H] \lesssim -4$) and under the low-FUV ($\lesssim 10^{-3}$)/CR fields ($\lesssim 0.1$ of the present-day Galactic disk levels). In addition, with a given metallicity, all the temperature evolution tracks with different FUV/CR intensities converge before the density range where efficient cooling by dust triggers the cloud

fragmentation. This demonstrates that in studying evolution of the dense cores, we need not care about the past ionization history except in the limited circumstances.

This paper is organized as follows. In Sec. 2, we describe the method of calculation and input physics in our model. In Sec. 3, the results for temperature evolution of low-metallicity clouds are presented and analysed. Finally, in Sec. 4, we conclude the paper by summarizing our findings.

2. Method of Calculation

We calculate the thermal evolution of low-metallicity clouds by using a one-zone model, which is based on that by Omukai (2000) and Omukai et al. (2005), but with some modifications, including (i) chemical reaction network and its rate coefficients are updated and (ii) effects of FUV and CR irradiation, specifically, heating by photoelectric emission of dust grains and by CR ionization, and photo- and CR-induced chemical reactions, are added. The physical quantities, i.e., temperature, density, chemical fraction, etc., calculated in this model are regarded as those at the center of the cloud. The quantities calculated by this model are known to reproduce well the central evolution by hydrodynamical calculations for low-metallicity clouds (Omukai, Hosokawa, & Yoshida 2010) as well as for primordial clouds under FUV irradiation (Shang, Bryan, & Haiman 2010).

Without strong magnetic or turbulent supports, the dynamical collapse of self-gravitating clouds is well described by the Larson-Penston type similarity solution (Larson 1969; Penston 1968). During the collapse, the cloud develops the core-envelope structure with homogeneous central region of nearly the Jeans length in size and the envelope where the density decreases with radius as $\propto r^{-2}$. By mimicking the above property of the Larson-Penston solution, we assume the density increases by

$$\frac{d\rho}{dt} = \frac{\rho}{t_{\text{col}}}, \quad (4)$$

where ρ is the density of the gas, and the collapse timescale $t_{\text{col}} = \sqrt{3\pi/32(1-f)G\rho}$ where f is the ratio of pressure gradient to gravity and given as a function of the effective equation of state (see Omukai et al. 2005). The temperature evolution is followed by solving the energy equation:

$$\frac{de}{dt} = -p \frac{d}{dt} \left(\frac{1}{\rho} \right) - \Lambda_{\text{net}}, \quad (5)$$

where the specific thermal energy is written as

$$e = \frac{1}{\gamma_{\text{ad}} - 1} \frac{kT}{\mu m_{\text{H}}}, \quad (6)$$

with the ratio of specific heat γ_{ad} , the temperature T , and the mean molecular weight μ , and, on the right-hand side, p is the pressure

$$p = \frac{\rho kT}{\mu m_{\text{H}}}, \quad (7)$$

and Λ_{net} is the net cooling rate per unit mass. The cooling processes included in Λ_{net} are the radiative cooling by the

¹ $[Z/H] \equiv \log(Z/Z_{\odot})$, where Z is the mass fraction of metals in the medium.

H Ly α transition, fine-structure line transitions of [CII], [CI], and [OI], and rotational (and also vibrational for H₂) transitions of molecules H₂, HD, CO, OH, and H₂O. In calculating the H₂ cooling rate, we also include the H₂-e and H₂-H⁺ collisional transitions in addition to the H₂-H and H₂-H₂ collisions since, in a highly ionized gas, collisions with electrons and protons can potentially dominate the H₂ excitation (Glover & Abel 2008). The newly added transition rates are taken from Draine, Roberge, & Dalgarno (1983) for the H₂-e collisions and Gerlich (1990) for the H₂-H⁺ collisions, following Glover & Abel (2008). The cooling rates by the other species are calculated as in Omukai et al.(2010). In evaluating the photon trapping effects, we use the column density $N_{\text{H}} = n_{\text{H}}\lambda_{\text{J}}$, recalling that the size of the core is about a Jeans length λ_{J} . The heating processes are those associated with the H₂ formation, photoelectric emission from the dust grains, and CR ionization. The heating rates by photoelectric emission of dust grains and by CR ionization are taken from Wolfire et al. (1995).

The chemical reactions among species composed of elements H, He, C, and O are solved. We consider the following 50 species as in Omukai et al.(2005): H, H₂, e⁻, H⁺, H₂⁺, H₃⁺, H⁻, He, He⁺, He⁺⁺, HeH⁺, D, D⁺, D⁻, HD, HD⁺, C, C₂, CH, CH₂, CH₃, CH₄, C⁺, C₂⁺, CH⁺, CH₂⁺, CH₃⁺, CH₄⁺, CH₅⁺, O, O₂, OH, CO, H₂O, HCO, O₂H, CO₂, H₂CO, H₂O₂, O⁺, O₂⁺, OH⁺, CO⁺, H₂O⁺, HCO⁺, O₂H⁺, H₃O⁺, H₂CO⁺, HCO₂⁺ and H₃CO⁺. The included reaction network among those species are updated from Omukai et al.(2005), whose reaction network is largely based on the UMIST database of Millar et al.(1997) in addition to the primordial-gas chemistry from several sources (e.g., Abel et al. 1997; Galli & Palla 1998). Our new network is based on the updated UMIST database of Woodall et al.(2007), supplemented by primordial-gas chemistry of Glover & Abel (2008). Specifically, we construct our chemical network as follows. First, we consider all the primordial-gas reactions in Glover & Abel (2008) except those involving doubly deuterated species D₂ and D₂⁺. For uncertain three-body H₂ formation rate, we choose the value recommended by Glover (2008). Then, from a large number of the reactions listed in Woodall et al. (2007), we take those involving the above 50 species only, but excluding the collider reactions, which become important only in higher density than our calculated range. For overlapping reactions between the two compilations, we use the rate coefficient presented in Glover & Abel (2008). Primordial-gas reactions not in Glover & Abel (2008) but in Woodall et al. (2007) are also considered. Finally, photodissociation of H₂ and HD is added (see below). Notable addition to our previous chemical model includes the photo- and cosmic-ray induced reactions as well as cosmic-ray induced photon reactions. The rate coefficients for CR-/photo-induced reactions by Woodall et al. (2007) are presented for those for the intensities in the Galactic disk, i.e., the CR primary ionization rate $\zeta_{\text{disk}} = 1.3 \times 10^{-17} \text{s}^{-1}$, and the FUV intensity with respect to the Draine field $G_0 = 1.7$ (Draine 1978), where the Habing parameter G_0 is defined

by the FUV flux in the range 6-13.6 eV normalized by $1.6 \times 10^{-3} \text{erg cm}^{-2} \text{s}^{-1}$ (Habing 1968). We thus rescale the coefficients in Woodall et al. (2007) for CR-induced reactions and photo-ionization/dissociation by multiplying the factor $\zeta/\zeta_{\text{disk}}$ and $G_0/1.7$, respectively. This scaling corresponds to the assumption that the FUV spectrum is the same as the Galactic field, which can be invalidated, for example, for the radiation field dominated by massive pop III stars with high ($\sim 10^5$ K) effective temperature. The photo-chemical reaction coefficients decrease exponentially with the visual extinction A_{V} owing to the shielding by dust grains. The visual extinction is related with the column density of the hydrogen nuclei as $A_{\text{V}} = 5.3 \times 10^{-22} N_{\text{H}} \text{cm}^{-2} (Z/Z_{\odot})$ under the assumption of grains with the same optical properties as in the solar neighborhood (Bohline et al. 1978; Rachford et al. 2009). For the photodissociation of H₂ and HD, and CO, in addition to the dust shielding, the shielding by H₂ becomes important. For H₂ photodissociation, we use the reaction rate by Draine & Bertoldi (1996)

$$k_{\text{H}_2\text{pd}} = 4.50 \times 10^{-11} f_{\text{sh}} \exp(-2.5A_{\text{V}}) G_0 \text{ s}^{-1}, \quad (8)$$

where the shielding factor f_{sh} are taken from Wolcott-Green & Haiman (2010). For the HD photodissociation, we use the same expression as H₂ (eq. 8), but the proper shielding factor for HD (Wolcott-Green & Haiman 2010). For the photodissociation of CO, we modify the reaction coefficients from Woodall et al. (2007) by including the shielding by H₂. We use the fit to Lee et al. (1996)'s results by Hosokawa & Inutsuka (2006), which is within 20 % accuracy for $N_{\text{H}_2} < 8 \times 10^{21} \text{cm}^{-2}$ although substantially worse at higher N_{H_2} :

$$k_{\text{COpd}} = 2.0 \times 10^{-10} \exp\left(-3.5A_{\text{V}} - \frac{N_{\text{H}_2}}{1.6 \times 10^{21} \text{cm}^{-2}}\right) (G_0/1.7) \text{ s}^{-1}.$$

We do not take the shielding of CRs into account. Although the CR shielding becomes important for column density $\gtrsim 29 \text{g cm}^{-2}$ (Umebayashi & Nakano 1986), the column density does not reach such high and the shielding does not have a large effect in our calculations.

The initial number density is taken at 0.1cm^{-3} , which is a typical value in the relic HII regions of the first stars (Yoshida et al. 2007). We consider two types of the initial conditions: (i) un-ionized condition: the initial temperature $T_{\text{ini}} = 1000 \text{K}$, the ionization degree $y_{\text{ini}}(\text{e}) = 3 \times 10^{-4}$, molecular fraction $y_{\text{ini}}(\text{H}_2) = 2 \times 10^{-5}$, and (ii) pre-ionized condition : $T_{\text{ini}} = 8000 \text{K}$, $y_{\text{ini}}(\text{e}) = 0.5$, $y_{\text{ini}}(\text{H}_2) = 0$. The un-ionized condition (i) is typical for the formation of the first stars (Yoshida et al. 2006), while the pre-ionized condition (ii) corresponds to the transitional state where the recombination is proceeding in the relic HII region (Yoshida et al. 2007a). The factor of a few variations in those initial chemical abundances do not alter the thermal evolution of gas presented below.

3. Results

3.1. No FUV/CR Cases

First, we see the cases with neither CR nor FUV field. Figure 1 presents the comparison of thermal evolution of low-metallicity gas in the un-ionized and pre-ionized cases.

The lower panel shows the results in un-ionized cases. In low densities ($\lesssim 10^4 \text{cm}^{-3}$), temperatures are almost the same for the clouds with $[Z/H] \leq -4$ as H_2 is the dominant coolant in this density/metallicity range. For higher metallicity, i.e., $[Z/H] \geq -3$, cooling by the C and O fine-structure transitions breaks this degeneracy: the temperature becomes lower for higher metallicity. In the higher density range, temperature tracks deviate from the $Z=0$ one also for $[Z/H] \lesssim -4$, owing to cooling by H_2 formed by the dust surface reaction, and by H_2O , both of whose amounts are dependent on metallicity.

Next we see the pre-ionized cases (upper panel). For $[Z/H] \lesssim -4$, HD dominates the cooling in $\lesssim 150\text{K}$, and thus the temperature tracks degenerate until $\sim 10^8 \text{cm}^{-3}$ where the gas is heated up to $\sim 300\text{K}$ by the exothermic three-body H_2 forming reaction. In comparison with the un-ionized clouds, which cool solely by H_2 , the temperature in the pre-ionized clouds is significantly lower in the metallicity range $[Z/H] \lesssim -4$, thanks to the HD cooling. This effect, efficient HD cooling in the pre-ionized gas, is well-known for the primordial gas, i.e., the pop III.2 star formation. For $\gtrsim 10^8 \text{cm}^{-3}$, the warm environment makes H_2 the more important coolant than HD, and thus the temperature tracks become the same as those in the un-ionized cases. With more metals ($[Z/H] \geq -3$), the cooling rate by the fine-structure lines exceeds that by HD. The temperatures are then similar in both un-ionized and pre-ionized cases, although slightly lower in the pre-ionized cases. In the case of $[Z/H] = -1$, the pre-ionized gas takes slightly longer time, i.e., higher density, to reach the CMB temperature of 30K . This just reflects the higher initial temperature in the pre-ionized case.

To summarize, below the metallicity $[Z/H] \simeq -3$, HD is the dominant coolant for $\lesssim 10^8 \text{cm}^{-3}$ in the pre-ionized gas, and the thermal evolution depends on the initial ionization state as is known for the pop III star formation. For higher metallicity, on the other hand, the fine-structure-line cooling becomes more important and the pre-ionization has little impact on the subsequent thermal evolution.

3.2. Cases only with FUV irradiation

Next we see the cases with external FUV irradiation but without CR incitation. Panels in the Figure 2 correspond to the cases with different metallicities $Z=0$ (*left-top*), $[Z/H] = -5$ (*right-top*), -4 (*left-middle*), -3 (*right-middle*), -2 (*left-bottom*) and -1 (*right-bottom*). In each panel, the solid and dashed lines indicate the un-ionized and pre-ionized cases, respectively, for five different FUV strengths, $D_0 \equiv G_0/1.7 = 0$ (*blue*), 10^{-3} (*green*), 10^{-2} (*orange*), 10^{-1} (*magenta*) and 1 (*red*). In the pre-ionized cases (*dashed*) with strong FUV fields ($D_0 \geq 0.1$), heating by the photoelectric emission and cooling by the Ly α

emission balances, and the temperature remains almost constant at the initial value of 8000K for a while. In the un-ionized cases (*solid*), the temperature increases adiabatically from the initial 1000K to several thousand K, depending on the strength of FUV field, since the photodissociation prevents the H_2 formation and its cooling. In both un-/pre-ionized cases, the temperature begins to fall down when the H_2 self-shielding against the photodissociation becomes effective for $[Z/H] \lesssim -3$. With high enough metallicity $[Z/H] \gtrsim -2$, the fine-structure-line cooling causes the temperature decrease before the H_2 is self-shielded.

As discussed in Sec. 3.1, without an FUV field, the thermal evolution of low-metallicity gas ($[Z/H] \lesssim -4$) bifurcates according to its initial ionization state. This still holds true in weak enough FUV cases (see the cases with $D_0 \leq 10^{-3}$). With higher FUV intensity ($D_0 \geq 10^{-2}$), however, the temperatures in un-ionized and pre-ionized cases quickly converge each other during the initial temperature-decreasing phase. The dependence on the initial ionization state immediately disappears. This is because sufficient HD for cooling is not formed in either un-ionized nor pre-ionized case: even in the pre-ionized cases, H_2 photodissociation by FUV field prevents the gas to cool $\lesssim 150\text{K}$, thereby quenching HD formation, which proceeds only in the low-temperature environments. For $[Z/H] \gtrsim -3$, as in no UV cases, the minimum temperatures are the same for pre-/ un-ionized cases and no effect of pre-ionization is observed during the subsequent thermal evolution.

It should be noted that, in all the cases, for $\gtrsim 10^8 \text{cm}^{-3}$, neither the initial ionization state nor the irradiating FUV strength affect the thermal evolution. This is because the H_2 fraction boosts up at $\sim 10^8 \text{cm}^{-3}$ by the three-body reaction and its differences due to different initial ionization or FUV field strength in lower densities are wiped out. For high metallicity cases $[Z/H] \geq -3$, this convergence of the thermal evolution occurs at even lower density since the H_2 cooling is only subordinate to the fine-structure-line cooling.

3.3. Cases also with CRs

Finally, we see the cases not only with FUV irradiation, but also with the CR incitation. In the solar neighborhood, the CR energy density is estimated, in terms of the primary ionization rate, to be $\zeta_{\text{disk}} \sim 10^{-17} \text{s}^{-1}$ (Webber & Yushak 1983), with about an order of magnitude uncertainty (e.g., Indrilo et al. 2007). Although the CR strength is, of course, far more uncertain in the early universe, about $1/100$ of the Galactic value $\zeta \sim 10^{-19} \text{s}^{-1}$ is claimed as an intergalactic CR field (Stacy & Bromm 2007). In this section, we regard the CR intensity as a free parameter and study cases with $\zeta = 10^{-19} \dots 10^{-17} \text{s}^{-1}$.

Figure 3 shows the weak CR cases of $\zeta = 10^{-19} \text{s}^{-1}$. At first glance, these results resemble very well with those without CRs shown in Figure 2. However, at very low-metallicity $[Z/H] \lesssim -4$ and at the same time with low FUV intensity $D_0 \lesssim 10^{-3}$, the temperature in the un-ionized

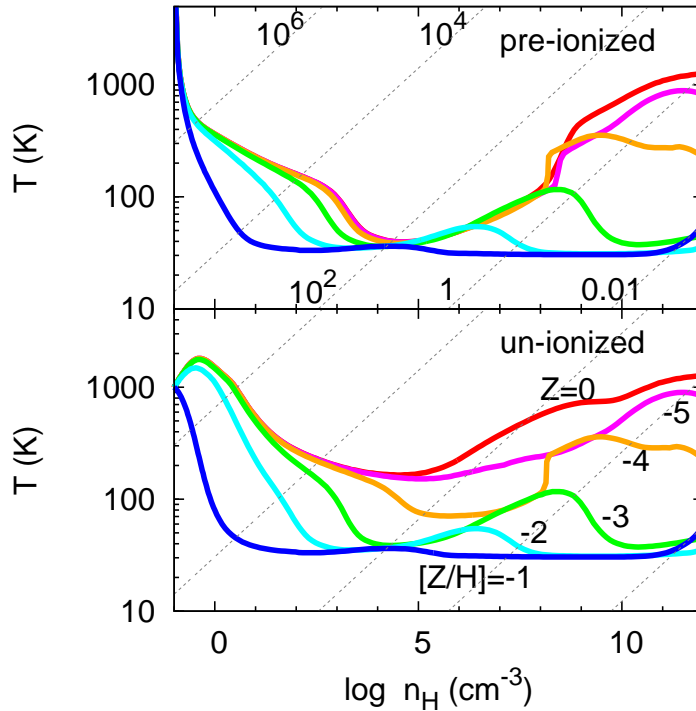


Fig. 1. Temperature evolution in clouds with six different metallicities ($Z=0$ (red), $[Z/H]=-5$ (magenta), -4 (orange), -3 (green), -2 (cyan), and -1 (blue)) against number density in the pre-ionized (upper panel) and for un-ionized (lower panel) cases. The cases with neither FUV nor CR incidence. The values of metallicities $[Z/H]$ are indicated by numbers in the lower panel. The thin dashed lines indicate the constant Jeans mass, whose value is shown by numbers in the upper panel.

cases is somewhat lower in the range of $10^5 - 10^7 \text{cm}^{-3}$ than in the no CR cases, because the CR ionization enables the HD cooling (c.f. Stacy & Bromm 2007). The cases with higher CR intensity $\zeta = 10^{-18}$ and 10^{-17}s^{-1} are presented in Figures 4 and 5, respectively. The latter CR value is as high as in the present-day Galactic disk. Most notably, with increasing CR strength, the pre-ionization effect becomes weaker. Without CR, the pre-ionization effect is clearly visible for clouds with low-metallicity $[Z/H] \lesssim -4$ and simultaneously with low FUV intensity $D_0 \lesssim 10^{-3}$ (Sec. 3.2). With increasing CR intensity, the differences among the pre-ionized and un-ionized cases diminish even in those cases. Recall that, without CR, the HD formation/cooling is operative only in the pre-ionized environment. With some CR incidence, CR ionization induces the HD formation/cooling even in the un-ionized condition. The differences in temperature evolution among pre-ionized and un-ionized cases thus become smaller for higher CR strength. Besides ionization, CRs also have the heating effect. This is clearly seen in Figures 4 and 5 as a rapid initial temperature rise in the un-ionized cases with metallicity $[Z/H] \lesssim -2$. For density $\gtrsim 10 \text{cm}^{-3}$, this effect is not visible compensated by efficient cooling.

4. Summary and Conclusion

We have studied the effect of pre-ionization, as well as the far-ultraviolet irradiation and cosmic-ray incidence, on the thermal evolution of low-metallicity star-forming gas. Our findings can be summarized as follows:

1. Without external FUV or CR irradiation, HD formation is promoted in the initially ionized (“pre-ionized”) clouds. This HD cooling makes the temperature in low-metallicity ($[Z/H] \lesssim -3$) clouds fall below the minimum value in the un-ionized gas attainable solely by H_2 cooling ($\approx 200\text{K}$). The temperature finally reaches a few 10 K, similar to the high-redshift CMB temperature. With more metals, regardless of HD formation/cooling, the gas is able to reach such low temperature by the fine-structure line cooling. In this case, the pre-ionization does not have impact on the thermal evolution.

2. Presence of a weak FUV field ($G_0 \sim 10^{-2}$) prevents the HD formation/cooling even in the pre-ionized gas. This is because of the H_2 photodissociation: without sufficient H_2 , the gas does not cool to $\lesssim 150\text{K}$, where the deuterium is rapidly converted to HD. In this case, the pre-ionization does not affect the subsequent thermal evolution of low-metallicity gas.

3. The cosmic-ray ionization as high as $\zeta \sim 10^{-18} \text{s}^{-1}$ in terms of the primary ionization rate, or $\sim 10\%$ of the solar neighborhood level, enables HD formation/cooling even in

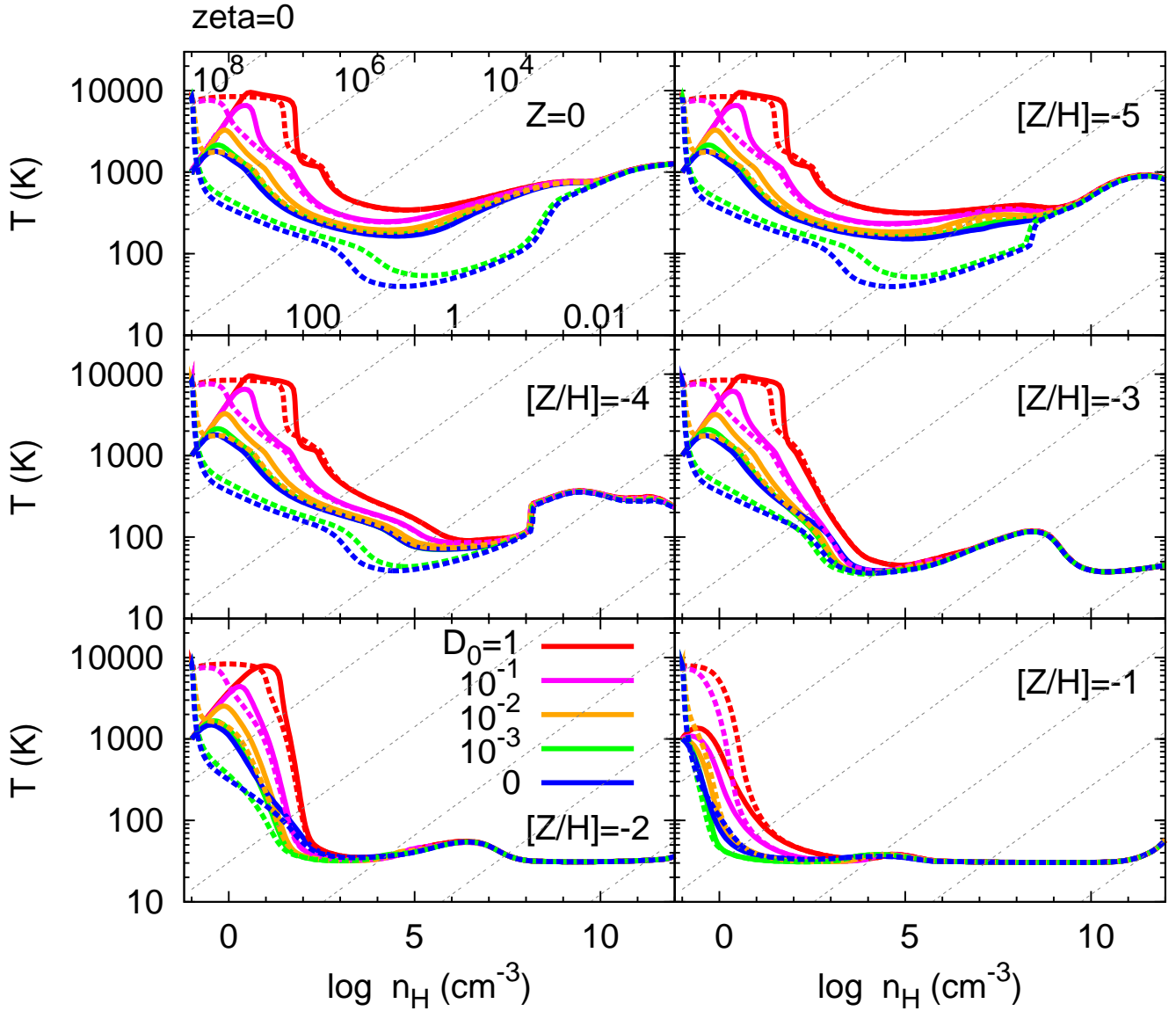


Fig. 2. Thermal evolution of low-metallicity clouds with FUV irradiation, but without CR incidence. Panels correspond to the cases with different metallicities $Z = 0$ (left-top), $[Z/H] = -5$ (right-top), -4 (left-middle), -3 (right-middle), -2 (left-bottom) and -1 (right-bottom). In each panel, the solid and dashed lines indicate the un-ionized and pre-ionized cases, respectively, for five different FUV strengths, $D_0 \equiv G_0/1.7 = 0$ (blue), 10^{-3} (green), 10^{-2} (orange), 10^{-1} (magenta) and 1 (red). The thin dashed lines indicate the constant Jeans mass, whose value is shown by numbers in the upper-left panel.

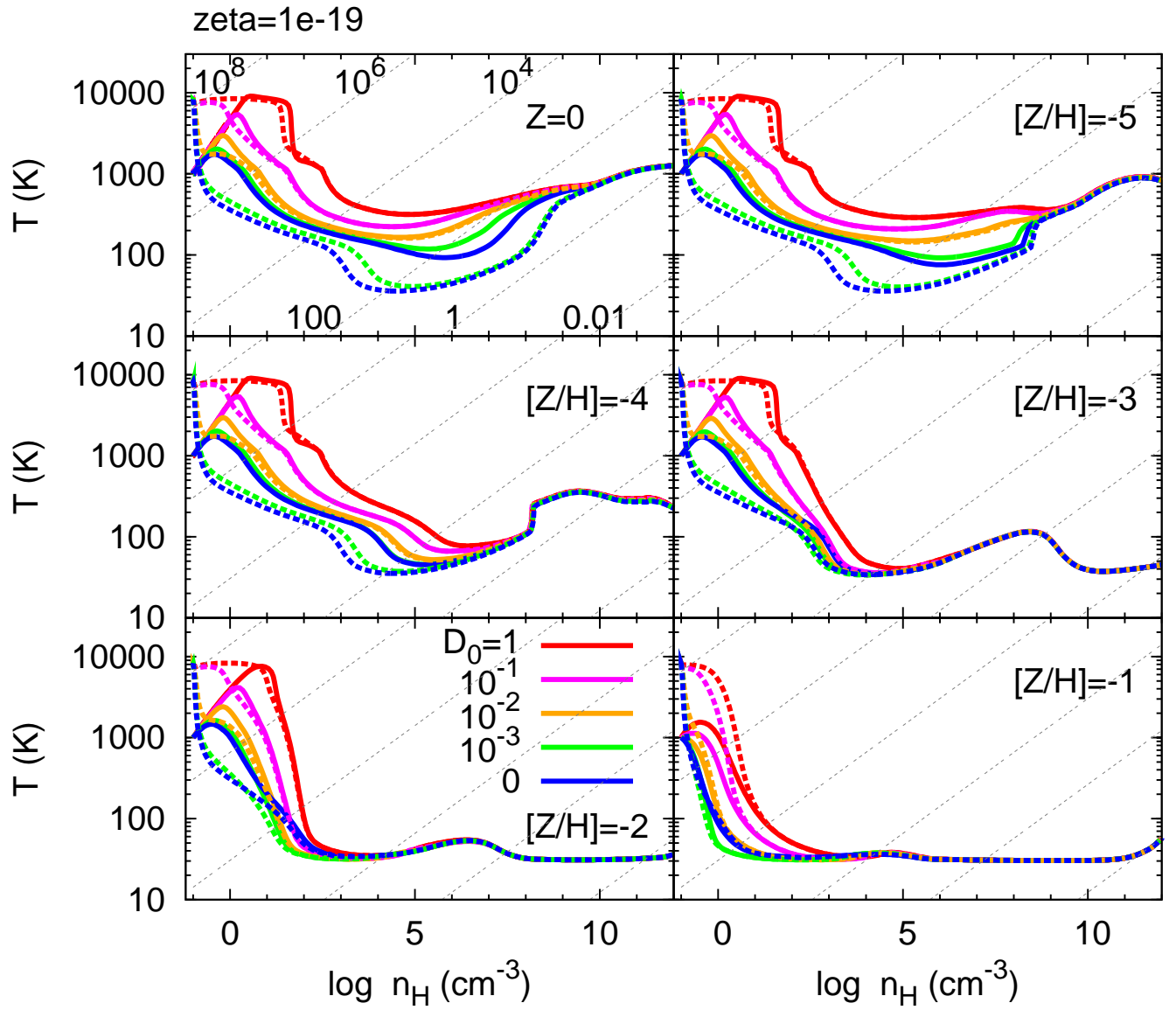


Fig. 3. Same as Figure 2 but with CR indication at the cosmic-ray primary ionization rate $\zeta = 10^{-19}\text{s}^{-1}$.

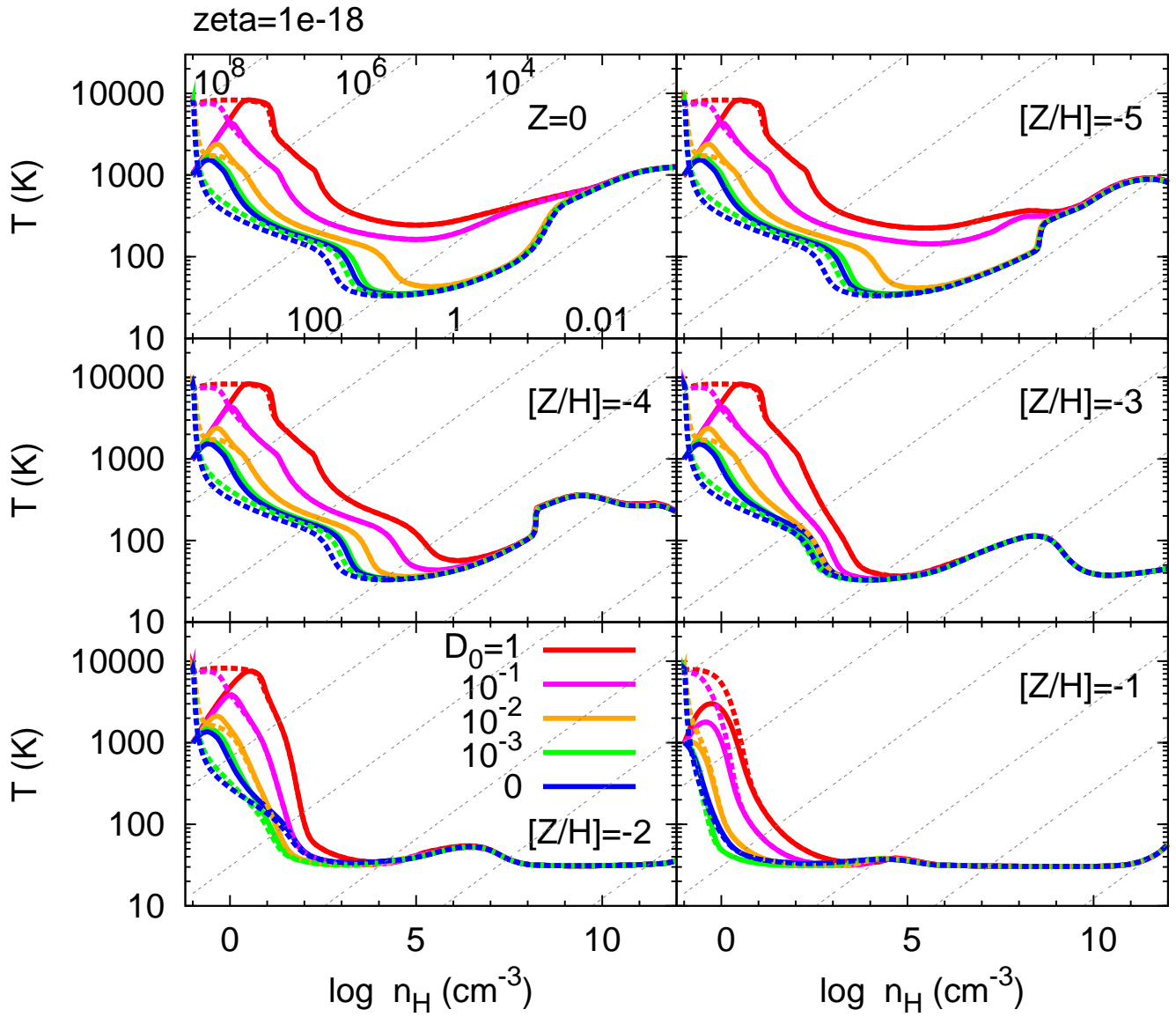


Fig. 4. Same as Figure 2 but for $\zeta = 10^{-18}\text{s}^{-1}$.

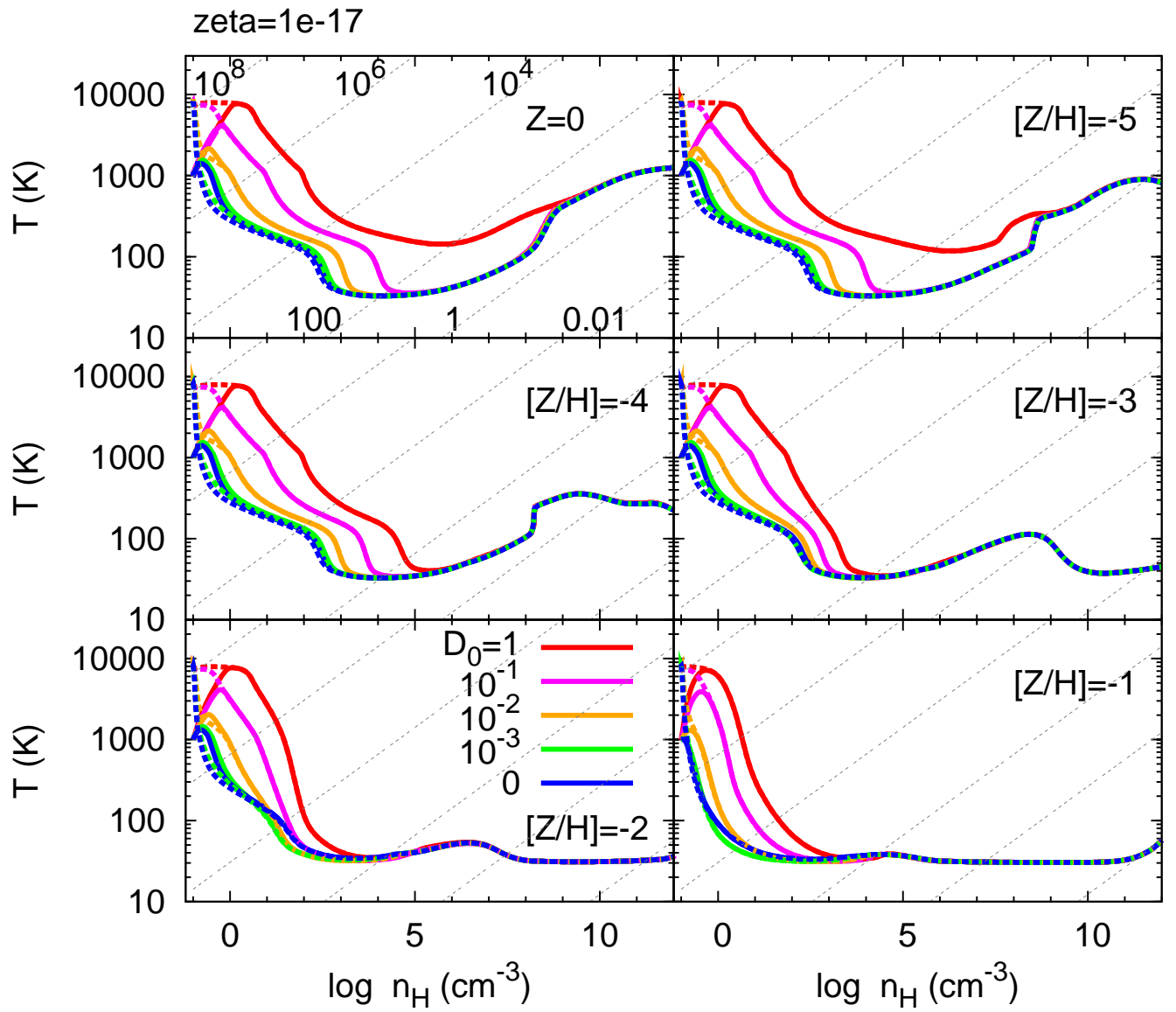


Fig. 5. Same as Figure 2 but for $\zeta = 10^{-17} \text{s}^{-1}$.

the un-ionized gas, thereby eliminating the pre-ionization effects even in very low-metallicity cases.

In summary, the pre-ionization has remarkable effects only in clouds with very low metallicity ($[Z/H] \lesssim -3$), and under low FUV ($G_0 \lesssim 10^{-2}$) or low CR ($\zeta \lesssim 10^{-18}$) fields.

In addition,

4. the effects of external FUV/CRs on thermal evolution vanishes until 10^8cm^{-3} in all the cases we studied.

The convergence of thermal evolution at high density has important consequence on the mass-scale of forming stars. In the framework of dynamical fragmentation, clouds fragments during efficient cooling phase, where the temperature decreases with density, while fragmentation hardly occurs in the temperature-increasing phase (Larson 1985, 2005; Li et al. 2003). The characteristic fragmentation mass-scales are thus set by the Jeans mass at the local minima of temperature. The low-metallicity clouds with $-5 \lesssim [Z/H] \lesssim -1$ has two temperature minima during the collapse; the first one in the lower-density ($\sim 10^3 - 10^5 \text{cm}^{-3}$) due to the metal or H_2 , HD line cooling, and the second one in the higher-density ($\sim 10^{10} - 10^{15} \text{cm}^{-3}$) due to the cooling by dust thermal emission. Since the location of the first lower-density temperature minimum is vulnerable to the external FUV radiation, the fragmentation mass-scale owing to the line cooling can vary from cloud to cloud depending on the intensity of surrounding FUV field. On the other hand, as the temperature evolution depends neither on the pre-ionization nor external FUV radiation for $\gtrsim 10^8 \text{cm}^{-3}$, the location of the temperature minimum by the dust cooling is robust. Thus, in studying the fragmentation by dust cooling we do not need to care about the external radiation. The results of numerical simulations for dust-induced fragmentation (e.g., Tsuribe & Omukai 2006, 2008; Clark et al. 2008; Dopcke et al. 2011) remain valid also in the external radiation field.

The author is very grateful for constructive comments by anonymous referee. This study is supported in part by the Grants-in-Aid by the Ministry of Education, Science and Culture of Japan (2168407, 21244021).

References

Abel, T., Anninos, P., Zhang, Y., & Norman, M. L. 1997, *NewA*, 2, 181
 Abel, T. G., Bryan, G., & Norman, M. L., 2002, *Science*, 295, 93
 Bakes, E. L. O., & Tielens, A. G. G. M. 1994, *ApJ*, 427, 822
 Bohlin, R. C., Savage, B. D., & Drake, J. F. 1978, *ApJ*, 224, 132
 Bromm, V., Coppi, P., & Larson, R. B., 2002, *ApJ*, 564, 23
 Bromm, V. & Loeb, A. 2003, *Nature*, 425, 812
 Bromm, V., & Loeb, A. 2004, *New A*, 9, 353
 Clark, P. C., Glover, S. C. O., & Klessen, R. S. 2008, *ApJ*, 672, 757
 Dopcke, G., Glover, S. C. O., Clark, P. C., & Klessen, R. S., 2011, *ApJ*, 729, L3
 Draine, B. T. 1978, *ApJS*, 36, 595

Draine, B. T., Roberge, W. G., & Dalgarno, A. 1983, *ApJ*, 264, 485
 Draine, B. T., & Bertoldi, F. 1996, *ApJ*, 468, 269
 Galli, D., & Palla, F. 1998, *A&A*, 335, 403
 Gerlich, D. 1990, *J. Chem. Phys.*, 92, 2377
 Glover, S. C. O. & Abel, T. 2008, *MNRAS*, 388, 1627
 Glover, S. C. O. 2008, *FIRST STARS III*, AIP Conference Proceedings, 25
 Habing, H. J. 1968, *BAN*, 19, 421
 Heger, A., & Woosley, S. E. 2002, *ApJ*, 567, 53
 Hosokawa, T. & Inutsuka, S.-i. 2006, *ApJ*, 646, 240
 Hosokawa, T., Omukai, K., Yoshida, N. & Yorke, H. W. 2011, *Science*, 334, 1250
 Indriolo, N., Geballe, T. R., Oka, T., & McCall, B. J., 2007, *ApJ*, 671, 1736
 Jappsen, A.-K., Glover, S. C. O., Klessen, R. S., & Mac Low, M.-M. 2007, *ApJ*, 660, 1332
 Kitayama, T., Yoshida, N., Susa, H., & Umemura, M. 2004, *ApJ*, 613, 631
 Larson, R. B. 1969, *MNRAS*, 145, 271
 Larson, R. B. 1985, *MNRAS*, 214, 379
 Larson, R. B. 2005, *MNRAS*, 359, 211
 Lee, H.-H., Herbst, E., Pineau des Forets, G., Roueff, E., Le Bourlot, J. 1996, *A&A*, 311, 690
 Li, Y., Klessen, R. S., & Mac Low, M.-M., 2003, *ApJ*, 592, 975
 Machida, M. N., Omukai, K., & Matsumoto, T., 2009, *ApJ*, 705, 64
 Machida, M. N., Tomisaka, K., Nakamura, F., & Fujimoto, M. Y. 2005, *ApJ*, 622, 39
 McKee C. F. & Tan, J. C. 2008, *ApJ*, 681, 771
 Mackey, J., Bromm, V., & Hernquist, L. 2003, *ApJ*, 586, 1
 McGreer, I. D., & Bryan, G. L. 2008, *ApJ*, 685, 8
 Millar, T. J., Farquhar, P. R. A., & Willacy, K. 1997, *A&AS*, 121, 139
 Nagakura, T. & Omukai, K. 2005, *MNRAS*, 364, 1378
 Nakamura, F. & Umemura, M. 2002, *ApJ*, 569, 549
 Omukai, K., Hosokawa, T., & Yoshida, N. 2010, *ApJ*, '22, 1793
 Omukai, K., & Nishi, R. 1998, *ApJ*, 508, 141
 Omukai, K., & Palla, F. 2003, *ApJ*, 589, 677
 Omukai, K. 2000, *ApJ*, 534, 809
 Omukai, K., Tsuribe, T., Schneider, R., & Ferrara, A. 2005, *ApJ*, 626, 627
 O'Shea, B., Abel, T., Whalen, D., & Norman, M. L. 2005, *ApJ*, 628, L5
 O'Shea, B. W., McKee, C. F., Heger, A., & Abel, T. 2008, in proceedings of "First Stars III", American Institute of Physics
 O'Shea, B. W., & Norman, M. L. 2008, *ApJ*, 673, 14
 Peebles, P. J. E. 1968, *ApJ*, 153, 1
 Penston, M. V. 1968, *MNRAS*, 144, 425
 Rachford, B. L., Snow, T. P., Destree, J. D. et al. 2009, *ApJS*, 180, 125
 Salvaterra, R., Ferrara, A., & Schneider, R. 2004, *New Astronomy*, 10, 113
 Sasaki, S., & Takahara, F. 1993, *PASJ*, 45, 655
 Schneider, R., Ferrara, A., Natarajan, P., & Omukai, K. 2002, *ApJ*, 571, 30
 Shang, C., Bryan, G. L., & Haiman, Z. 2010, *MNRAS*, 402, 1249
 Stacy, A. & Bromm, V. 2007, *MNRAS*, 382, 229
 Uehara, H. & Inutsuka, S.-i. 2000, *ApJ*, 531, L91
 Umebayashi, T. & Nakano, T. 1990, *MNRAS*, 243, 103
 Umeda, H., & Nomoto, K. 2002, *ApJ*, 565, 385
 Webber, W. R. & Yushak, S. M. 1983, *ApJ*, 275, 391

- Wolcott-Green, J., & Haiman, Z. 2011, MNRAS, 412, 2603
- Woodall, J., Agúndez, M., Markwick-Kemper, A. J. & Millar, T. J. 2007, A&A, 466, 1197
- Yoshida, N., Omukai, K., Hernquist, L., & Abel, T. 2006, ApJ, 652, 6
- Yoshida, N., Oh, S. P., Kitayama, T. & Hernquist, L. 2007a, ApJ, 663, 687
- Yoshida, N., Omukai, K., & Hernquist, L. 2007b, ApJ, 667, L117